European Journal of Technique

journal homepage: https://dergipark.org.tr/en/pub/ejt

Vol.11, No.1, 2021

# De-Orbiting Electro-Mechanical System Design for Micro Spacecraft

**Uğur Kesen**[1*]

[1*]Marmara University, Technology Faculty, Mechatronics Engineering Department, 34722, Goztepe, Istanbul, Turkey. (e-mail: ukesen@marmara.edu.tr).

ARTICLE INFO

Received: Apr., 04. 2021
Revised: May., 24. 2021
Accepted: May, 31. 2021

Keywords:
De-orbiting
Electro mechanic
Nano-micro spacecraft
Satellite

Corresponding author: *Uğur Kesen*

ISSN: *2536-5010* | e-ISSN: *2536-5134*

DOI: https://doi.org/10.36222/ejt.942123

## ABSTRACT

The number of small and micro satellites in Low Earth Orbit (LEO) is rapidly increasing. There is a risk of collision due to the lack of active orbital control of these satellites which also raises concerns about the debris. Existing low-orbit satellites pose dangers for new low-orbit satellites to be sent into orbit. A de-orbiting system to be activated at the end of the lifetime of the satellites is seen as the most effective solution to this danger. In this study, an electromagnetic satellite de-orbiting system is designed using aerodynamic principle. This system has been developed for a micro satellite with maximum edge dimensions of 100 cm. When the satellite lifetime is over, the system will be activated and will drop the satellite at the latest of 11 years. This system can de-orbit a micro satellite with a maximum weight of 50 kilograms. This system is activated with a command from the earth after the lifetime of the satellite is over. In this study, a de-orbiting electromechanical system (DES) is designed with an assumption of 750 km of satellite altitude and 98.4 degrees of orbital slope.

## 1. INTRODUCTION

In recent years, industry groups and universities all around the world launch an increasing number of micro satellites. Small satellites like CubeSat allow low-cost access to space. Several companies have proposed global broadband Internet networks provided by vast constellations of thousands of small satellites. [1]. A small spacecraft produced in accordance with the standards significantly reduces the development process and cost. At this stage, the most important problem is the pollution caused by expired satellites and the destruction of them. The existence of satellites, which have completed their lifetime and are now waste, poses a collision hazard for newly sent and active satellites. Out of 34,000 objects larger than 10 cm in orbit, only 20,000 have been cataloged [2, 3]. These cataloged objects include about 2000 active satellites, among which less than 1500 are maneuverable. These numbers are indicated in figure 1.

Everything else consists of orbital debris, large moons of the launch vehicles upper stages, mission-related objects, immobile parts from non-maneuverable fragmentation or collisions [4]. Non-trackable debris population is the primary risk and danger to successful operations in space. Objects that are too small to be cataloged in an orbital debris environment could cause a collision large enough to disable a satellite [5]. In a recent study, the authors propose establishing a new initiative called space environment management (SEM), consisting of both debris mitigation and debris remediation to reduce the risk of collision [6]. Another possible system used to avoid collisions is a sounding rocket system that will drag down the satellite and cause a deviation from the orbit [7]. Some technologies exist to increase the surface area of a CubeSat and accelerate orbit due to aerodynamic drag in low Earth orbit [8, 9]. There are also other studies that focus on use of lasers to re-orbit large orbital debris and spacecraft [10, 11]. Also, some other studies consider basic technologies of active removal of space debris from the geostationary orbit. This concept designed to take advantage of service spacecrafts by coupling them to a rigid arm to capture debris and tow them to graveyard orbit [12]. In another study, a solar sail was deployed to low Earth orbit and the sail membrane was used as a drag-sail to perform de-orbiting [13].

In this study, an electromagnetic satellite de-orbiting system is designed using aerodynamic principle. The electronic system operates a mechanical sailing module with the Sail module codes it receives from the earth. This electromechanical system will bring the micro satellite, with the maximum edge dimensions of 100 cm and a maximum weight of 50 kilograms, back to the earth at the latest of 11 years. In this study, a de-orbiting electromechanical system

(DES) is designed with an assumption of 750 km of satellite altitude and 98.4 degrees of orbital slope.

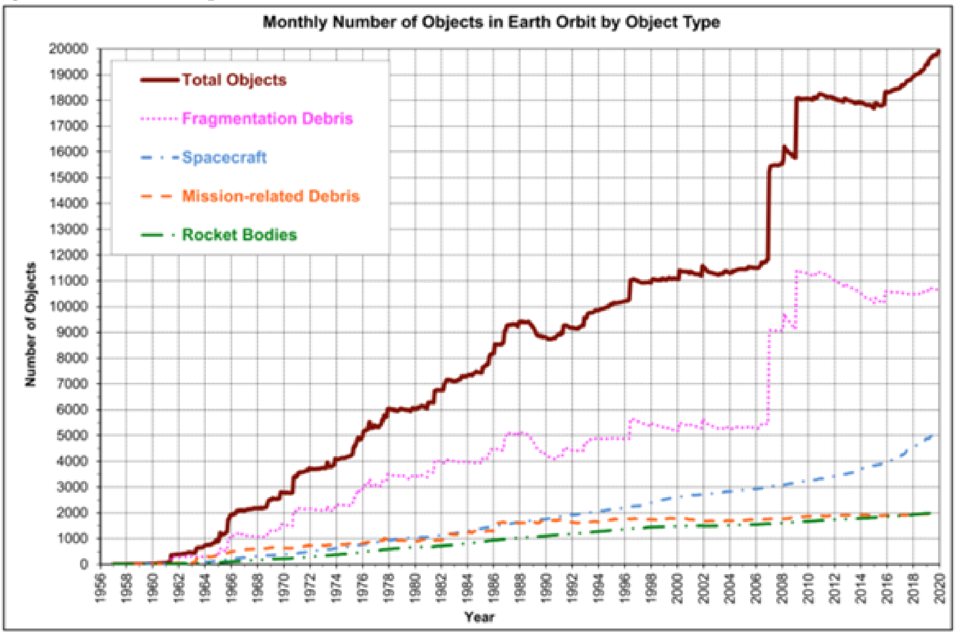


Figure 1. Number of cataloged objects in earth orbit by object type [4]

## 2. MATERIALS AND METHOD

The designed de-orbiting system uses aerodynamic principle. The system model block diagram is shown in Figure 2. The electronic circuit system breaks the line that will enable the operation of the mechanical system with the signal coming from the Earth to the micro satellite microprocessor. 4 different arms in the mechanical system are opened to activate a wide drop sail which will increase the dragging area. Each arm contains 3 different opening mechanism.

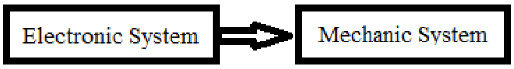


Figure 2. Electromechanical system model

The first opening mechanism opens a separate arm at 90 degrees from the satellite's body. After the first opening is completed, the second and third opening mechanisms begin to open simultaneously. After the opening is completed, the total surface area reaches 10.804 m2.

### 2.1. Design Equipments

The system is a design formed by the cooperation of many different equipment.

*Torsion Spring:* Torsion spring generates a force that will open the system 180 degrees. There are 2 torsion springs for each fan which sums up to a total of 8 torsion springs.

*Compression Springs:* After the fan is turned on, the compression springs push the fan, creating an additional 0.4 m2 drag area for each fan.

*Sail Hinge:* Sail hinge is used to open the sail arm.

Body Hinge: Body hinge joins the satellite and the fan system. The first opening occurs through the body hinges. It opens the main arm. Here, a spring with a wire thickness of 1.5 mm is used. The system contains a total of 4 hinges.

*Sail Wing:* It is used to open the arms in different directions. A torsion spring is also used here. Sail wing is connected to the body hinge.

*Arm and Arm Slot:* This area contains the compression springs. The compression spring pushes the inner lever which expands the sail area.

### 2.2. The Sail

The sail are the core components of the design. They increase the total aerodynamic drag area, increasing the satellite's fall time. The springs release the sails by moving the levers where the sails are connected. The unfolded sail is shown in figure 3. Sail will be turned off using origami techniques.

Figure 3. Sail and CAD design

#### 2.2.1. Sailing Material Kapton HN Film

Kapton HN general-purpose film has been successfully used in applications with temperatures ranging from -269°C (-452°F) to 400°C (752°F). Kapton HN film can be laminated, metallized, punched, formed or adhesive coated. For applications requiring an all-polyimide film with excellent property balance over a broad temperature range, Kapton HN is the preferred alternative. Kapton HN Film is shown in Figure 4. Physical and thermal properties of Kapton HN Film is shown table1 and table 2 [14].

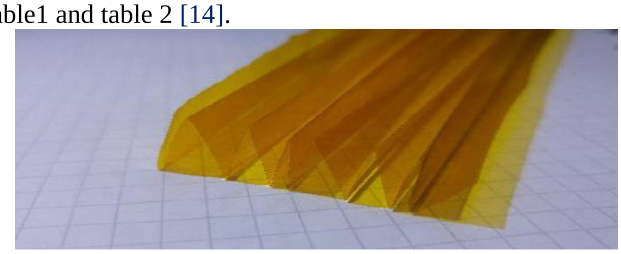

Figure 4. Kapton HN film

TABLE 1. Physical properties of Kapton HN film [14]

| Property | Unit | 75µm | 125µm |
|---|---|---|---|
| Ultimate Tensile Strength<br>At 23°C (73°F)<br>At 200°C (392°F) | psi<br>(MPa) | 33,5 (231)<br>20,0 (138) | 33,5 (231)<br>20,0 (138) |
| Density | g/cc | 1.42 | 1.42 |
| Tear Strength, Initial (Graves) | N (lbf) | 26.3 (1.6) | 46.9 (1.6) |

TABLE 2. Thermal properties of Kapton HN film [14]

| Property | Typical Value | Test Conditions |
|---|---|---|
| Thermal Coefficient of Linear Expansion | 20 ppm/°C (11 ppm/°F) | -14 to 38°C (7 to 100°F) |
| Specific Heat, J/g.K (cal/g·°C) | 1.09 (0.261) | |
| Shrinkage, %<br>30 min at 150°C<br>120 min at 400°C | 0.17<br>1,25 | |

## 2.2.2. Sailing Material Mylar Film

Mylar films are rugged, all-purpose films that are translucent in heavier gauges and clear in 48 through 92 gauges. They have a rough surface that allows for easy handling, adhesion, and processing. They're used in a wide variety of industrial settings. Physical and thermal properties of Mylar Film is shown table 3 and table 4. Mylar film is shown in Figure 5 [15].

TABLE 3. Physical properties of Mylar film [15]

| Property | Unit | Thickness (µm) |
|---|---|---|
| Tensile Strength MD | kpsi | 28 |
| Tensile Strength TD | kpsi | 34 |
| Elongation at Break MD | % | 125 |
| Elongation at Break TD | % | 100 |

TABLE 4. Thermal properties of Mylar film [15]

| Property | Unit | Thickness (µm) |
|---|---|---|
| Shrinkage MD (150°C) 30 min | % | 1.5 |
| Shrinkage TD (150°C) 30 min | % | 1.0 |

The system is completely switched to open conformation with the opening of the compression springs which activates DES. The steps of DES activation are shown in Figure 6.

Figure 5. Mylar film

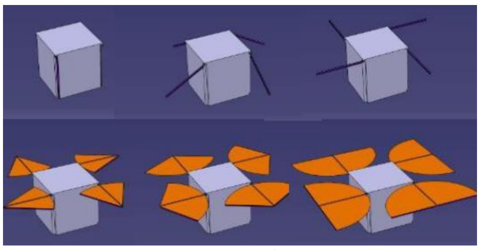

Figure 6. The steps of DES activation

## 2.3. Mechanism Design

During the lifetime of the satellite, the system will stay in a closed conformation. After the completion of its lifetime, the first part of the unfolding starts with the release of the torsion spring. The lines that keep the torsion spring taut are connected to a resistor which when heated burns the line causing the release of the torsion spring. After release, the torsion spring opens the main lever 90 degrees. The completion of first opening starts the second opening. The fan mechanism starts moving after the lines are burned. With this step, the sails start to unfold.

### 2.3.1 Mass Budget

It is important to keep the additional weight that DES will bring on the micro satellite as small as possible. Therefore, the mass budget of DES was calculated in table 5 and it was observed to be low.

Area Calculation: ((0.5x0.5x3.14)/2 + 0.4) x 4 + (0.5 x 0.5) = 3,42m2

TABLE 5. Mass budget

| Components | Mass (gr) | %20 Tolrance (gr) | Estimated Mass (gr) |
|---|---|---|---|
| Long spring (steel) | 7.47 | 1.49 | 8.96 |
| Tube (aluminum) | 74.61 | 14.92 | 89.53 |
| Inner lever (aluminum) | 49.15 | 9.83 | 58.99 |
| Wings x 2 (aluminum) | 48.17 | 9.63 | 57.81 |
| 180 degree opening hinge piece (aluminum) | 2.35 | 0.47 | 2.82 |
| 180 degree opening spring (steel) | 1.10 | 0.22 | 1.32 |
| First hinge (steel) | 53.12 | 10.62 | 63.75 |
| Kapton Film | 2.22 | 0.07 | 1.85 |
| Total x4 pieces | | | 1140.2 (gr) |

Because of its flexibility, low cost, and positive results at the end of its project life, the proposed design framework is favored. In order to develop an efficient DES system, we must consider whether it would work in space. At the end of its mission life, it must have an acceptable atmospheric re-entry period. The aerodynamic drag force concept is used to reduce the satellite's atmospheric re-entry period. This necessitates lowering the satellite's ballistic coefficient. The ballistic coefficient (BC) is used to describe spacecraft orbital decay, integrating the mass of the spacecraft, m, the region of its line-of-flight cross section, A, and the related drag coefficient, $C_d$, where:

$$BC = \frac{m}{A.C_d} \qquad (1)$$

Atmospheric drag is a major perturbing force for objects in Low-Earth Orbit. The drag force experienced by a spacecraft is determined by;

$$F_{aero} = -\frac{1}{2}.C_d.S \parallel V_{rel} \parallel V_{rel} \quad (2)$$

S is the spacecraft area projected along the direction of motion, $C_d$ is a dimensionless drag coefficient, q is the local atmospheric density, and Vrel is the relative velocity of the spacecraft with respect to the atmosphere.

By lowering the ballistic coefficient (BC), which is inversely proportional to $C_d$. A, we can reduce satellite atmospheric re-entry time. Therefore, Cd or satellite projected area along the direction of motion (A) must be increased. We create a DES concept based on a satellite in order to increase the projected area by using sail.

Advantages/Disadvantages of Kapton Film over Mylar Film;

- The tensile strength is higher than that of Mylar Film

EUROPEAN JOURNAL OF TECHNIQUE, Vol.11, No.1, 2021

- Elongation at break rate is less than Mylar
- It shrinks with less heat than Mylar

### 2.3.2 Operating System

The sail unfolding occurs through the heated resistors. For each sail to be unfolded, 4 resistors and 2 separate lines are required. In case one of the resistors malfunctions, the others will complete the operation. In case of a problem in the circuit and early heating of the resistors, one of the 2 lines will remain intact and prevent early unfolding. This way, the early unfolding of the sails is prevented, and the safety of the satellite is prolonged. The line system is shown in figure 7.

The line that holds the sails can resist a total of 37 kg of force. During the test, since real time waiting is not possible, the test was carried out by applying 37 kg of force to the line for 7 days. At the end of the test, no disintegration or expansion was observed on the line. This method was designed in the Istanbul Technical University Space Systems Design and Test Laboratory and was used in itüpsat, Türksat3Usat, BeEagleSat, Havelsat and Ubakusat satellites. And this line system has worked successfully in all satellites [16-18].

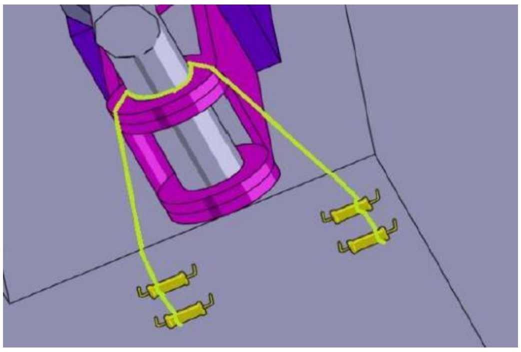

Figure 7. The line system

At room temperature, the 10-ohm resistor connected to the line was burned and disconnected in 7 seconds with 5V, 0.48A. Here, Nickel chrome wire, which can withstand higher temperatures, can be considered as a replacement for the resistor. Electronic circuit controlling the sailing system is shown in Figure 8.

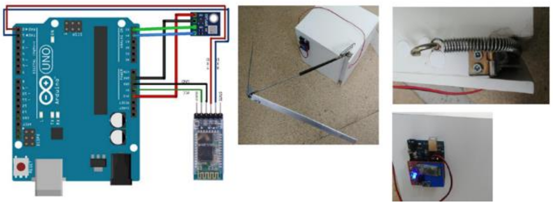

Figure 8. Electronic circuit controlling the sailing system

### 2.3.3 Lifetime Analysis

Satellite lifespan analysis was made with the analysis parameters given in Table 6. The results of the drop analysis for some scenarios are shown in Figure 9.

TABLE 6. Analysis parameters

| | |
|---|---|
| Semi-major axis | 7128 km |
| Orbital inclination | 98.4 degree |
| R.A.A.N | 30 degree |
| Argument pf Perigee | 210 degree |
| Mean Anomaly | 190 degree |
| Atmosphere model | |
| Cd | 2.2 |
| Cr | 1 |
| Solar Flux Estimates | CSSI |

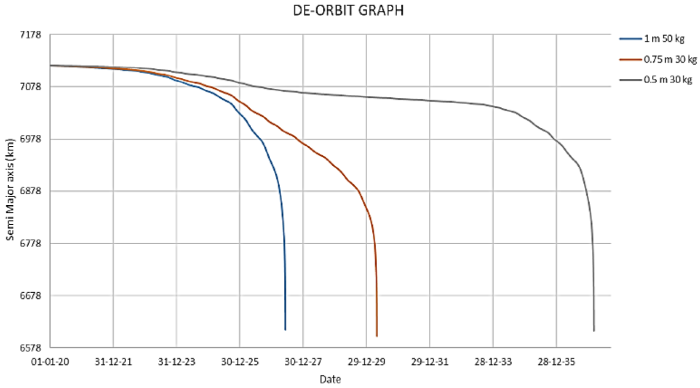


Figure 9. Drop Analysis for some scenarios

TABLE 7. Analysis results

| Scenario | Satellite Height (m) | Satellite Mass (kg) | Total Drag Area ($m^2$) | Total Drag Area Of The Satellite ($m^2$) | Life time (day) | Life time (year) |
|---|---|---|---|---|---|---|
| 1 | 1 | 50 | 10.804 | 11.804 | 2716 | 7.4 |
| 2 | 1 | 52 | 10.804 | 11.804 | 2875 | 7.9 |
| 3 | 1 | 40 | 10.804 | 11.804 | 2281 | 6.2 |
| 4 | 0.75 | 30 | 6.077 | 7.077 | 3772 | 10.3 |
| 5 | 0.75 | 50 | 6.077 | 7.077 | 6313 | 17.3 |
| 6 | 0.5 | 50 | 2.701 | 3.701 | 16496 | 45.2 |
| 7 | 0.5 | 40 | 2.701 | 3.701 | 7524 | 20.6 |
| 8 | 0.5 | 30 | 2.701 | 3.701 | 6276 | 17.2 |
| 9 | 1 | 50 | 0 | 1 | | 340 |

According to the results indicated in Table 7, the system we designed can drop a 1 cubic meter satellite of 50-kilogram mass in 7.4 years. The analysis was repeated with different satellite sizes and masses and a comparison was made. As can be seen from the table, If the length of one edge of the satellite is reduced to 0.5 meters, the time required to drop the satellite from an altitude of 750 km increases to 17 years. If a square satellite is designed with 1-meter edge length and the mass kept as 50 kg, the system meets the required conditions and drops the satellite before 11 years.

### 2.4 Sail Electronics Module

A simple electronic circuit that allows the sails to be unfolded was designed. The electronic circuit consists of Arduino microcontroller, pressure and height sensors. At a certain height and pressure value, the circuit enables the lines to break by heating the resistors. Thus, the release mechanism actuators work. The satellite's command receiver will interpret the sail module commands sent from the ground. It will send these commands to the sail electronics module over the bus. When the lifetime of the satellite ends or the satellite becomes unusable by any means, the command sent from the ground station to set the sails and de-orbit the satellite. The release mechanism and actuators have been tested with this circuit assembly. The electronic circuit controlling the sail opening system is shown in figure 8.

## 3. CONCLUSION

As a conclusion of this study, the system we designed can drop a 1 cubic meter satellite with 50 kilograms' mass in 7.4 years. The analysis was repeated for varying sizes and masses of satellites. The results suggest that this system can drop a micro satellite in a solar cycle. Also, altitude information data has been transferred successfully. The results vary for satellites with different sizes and masses. In addition, solar flux value is another important parameter that determines the life of the satellite. The system is applicable for various sizes of satellites. It is cheap and simple. At very high altitudes, the system is not effective enough due to low atmospheric density. Since the system is simple, inexpensive and has low mass, it can be preferred at altitudes such as 750 km. The drag area can be increased with minor improvements to the system.

## REFERENCES

**[1]** V. Braun, "Small Satellite Constellations and End-of-Life Deorbit Considerations." Handbook of Small Satellites: Technology, Design, Manufacture, Applications, Economics and Regulation, 2019, pp 1-23.

**[2]** C. Bonnal, D. McKnight, C. Phipps, C. Dupont, S. Missonnier, L. Lequette, M. Merle, S. Rommelaere, "Just in Time Collision Avoidance – a Review". Acta Astronautica, 170, 2020, pp 637-651.

**[3]** A. Chandra, J. Thangavelautham, "De-Orbiting Small Satellites Using Inflatables", in The 19th Advanced Maui Optical and Space Surveillance Technologies Conference. vol. 1 Maui, Hawai, 2018, pp 1-11.

**[4]** "Https://Orbitaldebris.Jsc.Nasa.Gov", (Last access: 25th September 2020)

**[5]** D. J. Kessler, B. G. Cour-Palais, "Collision Frequency of Artificial Satellites: The Creation of a Debris Belt." Journal of Geophysical Research: Space Physics, 83, 1978, pp 2637-2646.

**[6]** D. McKnight, T. Maclay, "Space Environment Management: A Common Sense Framework for Controlling Orbital." Debris Risk. Proc. AMOS, 2019.

**[7]** A. Jarry, C. Bonnal, C. Dupont, S. Missonnier, L. Lequette, F. Masson, "Srm Plume: A Candidate as Space Debris Braking System for Just-in-Time Collision Avoidance Maneuver." Acta Astronautica, 158, 2019, pp 185-197.

**[8]** D. Guglielmo, S. Omar, R. Bevilacqua, L. Fineberg, J. Treptow, B. Poffenberger, Y. Johnson, "Drag Deorbit Device: A New Standard Reentry Actuator for Cubesats." Journal of Spacecraft and Rockets, 56, 2019, pp 129-145.

**[9]** D. Turse, P. Keller, R. Taylor, M. Reavis, M. Tupper, C. Koehler, "Flight Testing of a Low Cost De-Orbiting Device for Small Satellites.", in The 42nd Aerospace Mechanism Symposium. vol. 1 Greenbelt, Maryland, 2014, pp 183-188.

**[10]** C. R. Phipps, C. Bonnal, "A Spaceborne, Pulsed Uv Laser System for Re-Entering or Nudging Leo Debris, and Re-Orbiting Geo Debris." Acta Astronautica, 118, 2016, pp 224-236.

**[11]** C. R. Phipps, "L′Adroit – a Spaceborne Ultraviolet Laser System for Space Debris Clearing." Acta Astronautica, 104, 2014, pp 243-255.

**[12]** A. Vnukov, T. Balandina, "Effectiveness Analysis of Active Space Debris Removal Technologies for the Geostationary Orbit." International Conference Aviamechanical engineering and transport (AVENT), 2018.

**[13]** S. A. Song, Y. Yoo, C. G. Han, S. Koo, J. Suk, S. Kim, "System Design of Solar Sail Deployment and Its Effect on Attitude Dynamics for Cube Satellite Cnusail-1", The Asia-Pacific International Symposium on Aerospace Technology (APISAT-2014), Shanghai, China, 2014, pp 24-26.

**[14]** "Https://Www.Dupont.Com/Content/Dam/Dupont/Amer/Us/En/Products/Ei-Transformation/Documents/Dec-Kapton-Hn-Datasheet.Pdf", (Last access: 25th September 2020)

**[15]** "Https://Laminatedplastics.Com/Mylar.Pdf", (Last access: 25th September 2020)

**[16]** A. R. Aslan, M. E. Bas, M. S. Uludag, S. Turkoglu, I. E. Akyol, M. D. Aksulu, E. Yakut, M. Suer, B. Karabulut, A. Sofyali, "The Integration and Testing of Beeaglesat", The 6th Nano-Satellite Symposium (NSAT), Kobe, Japan, 2015, pp 1-7.

**[17]** P. Acar, M. Nikbay, A. R. Aslan, "Design Optimization of a 3-Unit Satellite De-Orbiting Mechanism", ESA Small Satellites Systems and Services the 4S Symposium, 2012, pp 4-8.

**[18]** M. Cihan, O. O. Haktanir, I. Akbulut, A. R. Aslan, "Flight Dynamic Analysis of Itupsat1", International Workshop on small satellites, new missions and new technologies, 2008.

## BIOGRAPHIES

**Uğur KESEN** He received the BSc., and MSc. diploma in Electronic and Telecommunication Engineering from the Yıldız Technical University in 1990 and 1993 respectively, and PhD degrees in Graduate School of Science from Marmara University in 2001. He was engaged in research and project on the optical fibers telecommunication and artificial neural networks.